Optimal Control and Transcritical Bifurcation of a Prey-Predator Model with Disease Transmission Among the Prey Species, Beddington-Deangelis Functional Response and Prey Refuge

OGBU FAMOUS IMAGA[1,2], NIKOS MASTORAKIS[2]
[1]Department of Mathematics
Covenant University
Canaanland, Ota
NIGERIA

[2]Technical University of Sofia
English Language Faculty of Engineering,
Clement Ohridski 8, Sofia 1000,
BULGARIA

Abstract: - An eco-epidemiological prey-predator model incorporating disease transmission within the prey population, a Beddington-DeAngelis functional response, and a prey refuge mechanism was studied in this work. The mathematical well-posedness of the system was established by proving the existence, uniqueness, positivity, and uniform boundedness of its solutions. Five distinct biologically relevant ecological equilibrium points were identified and their local stability was evaluated using the Jacobian matrix and Routh-Hurwitz criteria. By constructing a suitable Lyapunov function, we demonstrated that the interior coexistence equilibrium point is globally asymptotically stable. Furthermore, we utilized Sotomayor's theorem to determine the explicit threshold values and verify the occurrence of transcritical bifurcations at key boundary equilibria. To mitigate disease spread and balance the ecosystem, we proposed an optimal control framework incorporating three time-dependent strategies: treatment, vaccination, and prey refuge enhancement. We characterize the optimal control paths using Pontryagin's Minimum Principle. Finally, numerical simulations were presented to validate the analytical results. The simulations reveal that applying a high economic terminal penalty effectively prevents disease relapse, steering the habitat toward long-term disease eradication and a thriving predator-prey environment.

Key-Words: - Eco-epidemiology, Beddington-DeAngelis functional response, Prey refuge, Transcritical bifurcation, Optimal control, Lyapunov stability.

Received: May 21, 2026. Revised: July 23, 2026. Accepted: August 25, 2026. Published: November 25, 2026.

1 Introduction

Mathematical models play an important role in understanding, analyzing and predicting the behaviour of many real-life systems in diverse fields like eco-epidemiology, epidemilogy and ecology [1], [2]. The modeling of prey-predator systems that involve complex ecological factors such as disease transmission among the prey species, predator interference and prey refuge is a complex branch of mathematical ecology [1]. Although researchers have considered individual components and different combinations, research seeking to unify the different components in real-time across different research fields is gaining momentum.

Infectious diseases play an important role in altering the biomass of both predators and preys in an ecosystem. Many studies have added disease dynamics into prey-predator interactions in order to understand how to efficiently manage the spread of infectious diseases [3], [4]. Some studies have focused on diseases among preys [5], [6], [7], while others investigated infections among predators [8], [9].

The Beddington-DeAngelis functional response is especially relevant in these unified frameworks. Unlike simpler models, it incorporates mutual interference among predators, thereby acknowledging that a predator's feeding rate can be restricted by encounters with other predators [10], [11], [12], [13]. In [13], the authors showed that predator interference stabilizes the interior equilibrium point and prevents uncontrolled chaotic oscillations at low population densities. Concurrently, a portion of the prey population is

shielded from predation by providing a prey refuge, which is a safe haven. This influences the population stability and dynamics significantly [14], [15], [16], [17], [18], [19], [20]. Different formulations have been used in the studying prey refuge, these includes constant prey refuge [17], [21], [22], proportional refuge [23], [24], or saturated or incorporate variable prey refuge [25], [26], [27]. Prey refuges prevent total species extinction, ensuring the permanence and boundedness of the ecosystem [15], in addition, if the prey refuge size is greater than a certain threshold, the prey refuge can have a significant influence on the stability of the dynamic system by turning oscillations into a stable equilibrium [16].

Bifurcation theory studies how a small parameter change alters long-term structure of an ecosystem. A transcritical bifurcation occurs when an equilibrium point exchanges stability with another as a parameter crosses a critical threshold [28], [29]. Certain parameters like the prey birth rate, disease transmission rate, or refuge capacity can trigger sudden emergence or extinction of species leading to the occurrence transcritical bifurcation [15], [28], [30].

Optimal control strategies are interventions applied to complex systems to manage the outbreak of infectious diseases in order to prevent the collapse of the ecosystem. In [30], the authors established that combining bifurcation insights and optimal control allows administrators to steer a system away from dangerous thresholds towards stable disease free states.

Though there is extensive literature on individual ecological mechanisms, a few studies have combined a Beddington-DeAngelis functional response with prey refuge constraints and disease dynamics under a single framework that simultaneously analyzes transcritical bifurcations and multi-strategy optimal controls. In this paper, we introduce and rigorously analyzes an eco-epidemiological prey-predator model featuring disease transmission within the prey population, a Beddington-DeAngelis functional response, and a prey refuge mechanism. By providing both qualitative bifurcation analysis and a time-dependent optimal control framework, this work provides a realistic, and integrated toolkit for ecosystem preservation and disease management.

2 Mathematical Model

In this work, we consider an eco-epidemiological habitat with two prey populations with disease transmission among the prey population and a single predator population where the predator feeds the prey. The model is represented by

$$\begin{aligned}
\dot{p_s} &= rp_s\left(1-\frac{p_s+p_i}{K}\right)-\beta p_s p_i \\
&\quad -\frac{\nu_s(1-\sigma_s)p_s z}{1+h(\nu_s(1-\sigma_s)p_s+\nu_i(1-\sigma_i)p_i)+\tau z}, \\
\dot{p_i} &= \beta p_s p_i-(\phi_i+\rho)p_i \\
&\quad -\frac{\nu_i(1-\sigma_i)p_i z}{1+h(\nu_s(1-\sigma_s)p_s+\nu_i(1-\sigma_i)p_i)+\tau z}, \\
\dot{z} &= -\delta z \\
&\quad +\frac{\zeta z[\nu_s(1-\sigma_s)p_s+\nu_i(1-\sigma_i)p_i]}{1+h(\nu_s(1-\sigma_s)p_s+\nu_i(1-\sigma_i)p_i)+\tau z},
\end{aligned} \tag{1}$$

subject to the initial conditions $y_i(0) \geq 0$, $i = 1, 2$, $z(0) \geq 0$. The biological significance of all the parameters is stated in table 1 below

Table 1: Biological significance of parameters

Parameter	Description
$p_s(t), p_i(t)$	population of susceptible and infected prey respectively
$z(t)$	population of the predator
r	prey natural growth rate
β	the rate of disease transmission
ν_s, ν_i	attack rates of susceptible and infected prey respectively
σ_s, σ_i	susceptible and infected refuge prey respectively
h	handling time
δ	predator death rate
ζ	conversion rate
τ	predator interference
ϕ_i	natural mortality rate of infected prey
ρ	instantaneous mortality rate as a result of infection

Source: Created by the Authors

3 Qualitative Analysis of the Mathematical Model

In this section, The existence of solutions to the mathematical model will be considered. We will also show that our model well-posed and functions properly by showing that all of its solution in $\mathbb{R}^3$ are non-negative and bounded. The equilibrium points will also be obtained while an analysis of the local and global stability will be conducted. These are to give a better understanding of how a predator-prey system is affected by infectious diseases.

3.1 Existence of Solutions of the Dynamical System

We will demonstrate the existence of solutions of the system of equation (1) together with the initial conditions in $\mathbb{R}^3_+$.

Theorem 1. dynamical system (1) together with the initial conditions has a unique solution in $\Omega = \{(p_s, p_i, z) \in \mathbb{R}^3_+\}$.

Proof. We will rewrite (1) as follow

$$\begin{aligned} g_1 &= rp_s\left(1-\frac{p_s+p_i}{K}\right)-\beta p_s p_i \\ &\quad -\frac{\nu_s(1-\sigma_s)p_s z}{1+h(\nu_s(1-\sigma_s)p_s+\nu_i(1-\sigma_i)p_i)+\tau z}, \\ g_2 &= \beta p_s p_i-(\phi_i+\rho)p_i \\ &\quad -\frac{\nu_i(1-\sigma_i)p_i z}{1+h(\nu_s(1-\sigma_s)p_s+\nu_i(1-\sigma_i)p_i)+\tau z}, \\ g_3 &= -\delta z \\ &\quad +\frac{\zeta z[\nu_s(1-\sigma_s)p_s+\nu_i(1-\sigma_i)p_i]}{1+h(\nu_s(1-\sigma_s)p_s+\nu_i(1-\sigma_i)p_i)+\tau z}. \end{aligned} \tag{2}$$

For $g=(g_1,g_2,g_3)$ and $u=(p_s,p_i,z)$, all the partial derivatives of the Jacobian matrix $\frac{\partial g}{\partial u}$ exists and are continuous and bounded in Ω. Hence, by the Derrick and Grossman theorem [31], a unique solution of (1) exists. This concludes the proof of existence of solution. □

3.2 Positivity of Solution the Dynamical System

Here, we will establish that our model is epidemiologically significant by demonstrating that the solutions of the system will remain positive with initial data greater than or equal to zero and for all $t \geq 0$.

Theorem 2. The solutions of the system of equations (1) are non-negative for positive initial condition and $t > 0$.

Proof. Let

$$\begin{aligned} A(p_s,p_i,z) &= r\left(1-\frac{p_s+p_i}{K}\right)-\beta p_i \\ &\quad -\frac{\nu_s(1-\sigma_s)z}{1+h(\nu_s(1-\sigma_s)p_s+\nu_i(1-\sigma_i)p_i)+\tau z}, \end{aligned}$$

$$\begin{aligned} B(p_s,p_i,z) &= \beta p_s-(\phi_i+\rho) \\ &\quad -\frac{\nu_i(1-\sigma_i)z}{1+h(\nu_s(1-\sigma_s)p_s+\nu_i(1-\sigma_i)p_i)+\tau z}, \end{aligned}$$

and

$$\begin{aligned} D(p_s,p_i,z) &= -\delta \\ &\quad +\frac{\zeta[\nu_s(1-\sigma_s)p_s+\nu_i(1-\sigma_i)p_i]}{1+h(\nu_s(1-\sigma_s)p_s+\nu_i(1-\sigma_i)p_i)+\tau z}, \end{aligned}$$

then 1 can be re-written as

$$\begin{aligned} p_s' &= p_s A(p_s,p_i,z), \quad p_s(0)\geq 0 \\ p_i' &= p_i B(p_s,p_i,z), \quad p_i(0)\geq 0 \\ z' &= zD(p_s,p_i,z), \quad z(0)\geq 0. \end{aligned} \tag{3}$$

The functions $p_sA(p_s,p_i,z)$, $p_iB(p_s,p_i,z)$ and $zD(p_s,p_i,z)$ are continuous by definition and locally Lipschitzian in $\mathbb{R}^3_+$. For $t_0 > 0$, a unique solution of (1) exists in the interval $[0,+\infty)$. We obtain from (3),

$$\begin{aligned} p_s' &= p_s(0)e^{\int_0^t A(p_s(s),p_i(s),z(s))ds}\geq 0, \quad p_s(0)\geq 0 \\ p_i' &= p_i(0)e^{\int_0^t B(p_s(s),p_i(s),z(s))ds}\geq 0, \quad p_i(0)\geq 0 \\ z' &= z(0)e^{\int_0^t D(p_s(s),p_i(s),z(s))ds}\geq 0, \quad z(0)\geq 0. \end{aligned}$$

The proof of positivity of solution to the model is concluded. □

3.3 Boundedness Of the Dynamical System

In the study of theoretical ecoepidemiology, boundedness is a vital requirement for a dynamical system to be biologically valid. In this subsection, we show that our model is biologically valid by demonstrating that it is bounded.

Theorem 3. For $t > 0$ and for any $\epsilon > 0$, the solutions of (1) starting in $\mathbb{R}^3_+$, are uniformly bounded in the positively invariant interval $\Omega = \left\{(p_s,p_i,z)\in\mathbb{R}^3_+ : 0 < P(t) \leq \frac{K(r+\mu)^2}{4\mu r}+\epsilon\right\}$.

Proof. Assuming that $(p_s(t),p_i(t),z(t))$ is a solution of (1) with initial conditions greater than or equal to zero, consider the function $P(t) = p_s(t)+p_i(t)+\frac{1}{\zeta}z(t)$, then

$$\begin{aligned} \frac{dP}{dt} &= \frac{dp_s}{dt}+\frac{dp_i}{dt}+\frac{1}{\zeta}\frac{dz}{dt} \\ &= rp_s\left(1-\frac{p_s+p_i}{K}\right)-(\phi_i+\rho)p_i-\frac{\delta z}{\zeta} \\ &\leq rp_s(K-p_s)-(\phi_i+\rho)p_i-\frac{\delta z}{\zeta} \end{aligned}$$

For a constant $\mu > 0$, if $\mu < \min\{\phi_i+\rho,\delta\}$, then from the above inequality

$$\frac{dP}{dt}+\mu P \leq \frac{K(r+\mu)^2}{4r}. \tag{4}$$

Solving (4) by Gronwall's inequality gives

$$0 < P(t) \leq \frac{K(r+\mu)^2}{4\mu r}(1-e^{-\mu t}) + P(p_s(0), p_i(0), z(0))e^{-\mu t}.$$

As $t \to \infty$, we get for any $\epsilon > 0$

$$0 < P(t) \leq \frac{K(r+\mu)^2}{4\mu r} + \epsilon.$$

The proof of boundedness of solution to the model is concluded. □

3.4 Equilibrium Points of the Model

The equilibrium points of the dynamical system (1) is obtained by solving the equations

$$\begin{aligned} & rp_s\left(1-\frac{p_s+p_i}{K}\right) - \beta p_s p_i \\ & - \frac{\nu_s(1-\sigma_s)p_s z}{1+h(\nu_s(1-\sigma_s)p_s+\nu_i(1-\sigma_i)p_i)+\tau z} = 0, \\ & \beta p_s p_i - (\phi_i+\rho)p_i \\ & - \frac{\nu_i(1-\sigma_i)p_i z}{1+h(\nu_s(1-\sigma_s)p_s+\nu_i(1-\sigma_i)p_i)+\tau z} = 0, \\ & -\delta z \\ & + \frac{\zeta z[\nu_s(1-\sigma_s)p_s+\nu_i(1-\sigma_i)p_i]}{1+h(\nu_s(1-\sigma_s)p_s+\nu_i(1-\sigma_i)p_i)+\tau z} = 0. \end{aligned} \tag{5}$$

Therefore the dynamical system (1) has the following five (5) equilibrium points:

(i) Extinction (Trivial) equilibrium point $B_0 = (0,0,0)$.

(ii) Disease-free prey (axial) equilibrium point $B_1 = (K,0,0)$.

(iii) Prey only endemic equilibrium point $B_2 = \left(\frac{\phi_i+\rho}{\beta}, \frac{r\left(K-\frac{\phi_i+\rho}{\beta}\right)}{r+\beta K}, 0\right)$ where $K > \frac{\phi_i+\rho}{\beta}$.

(iv) Disease free, predator-prey equilibrium point $B_3 = (p_s^-, 0, z^-)$ where
$p_s^- = \frac{K}{2r\zeta}\left(r\zeta - \frac{(\zeta-\delta h)\nu_s(1-\sigma_s)}{\tau} + \sqrt{\left[\frac{(\zeta-\delta h)\nu_s(1-\sigma_s)}{\tau} - r\zeta\right]^2 + \frac{4r\zeta\delta}{K\tau}}\right)$, and
$z^- = \frac{1}{\tau}\left[\left(\frac{\zeta}{\delta}-h\right)\nu_s(1-\sigma_s)p_s^- - 1\right]$.

(v) Coexistence or endemic equilibrium point $B_4 = (p_s^-, p_i^-, z^-)$ satisfy the equations:

$$r\left(1-\frac{p_s^-+p_i^-}{K}\right) - \beta p_i^- - \frac{\nu_s(1-\sigma_s)z^-}{M} = 0,$$

$$\beta p_s^- - (\phi_i+\rho) - \frac{\nu_i(1-\sigma_i)z^-}{M} = 0,$$

$$-\delta + \frac{\zeta[\nu_s(1-\sigma_s)p_s^- + \nu_i(1-\sigma_i)p_i^-]}{M} = 0$$

where
$M = 1+h(\nu_s(1-\sigma_s)p_s^- + \nu_i(1-\sigma_i)p_i^-) + \tau z^-$.

3.4.1 Local Stability Analysis of Equilibrium Points

The local stability can be obtained through the use of the Jacobian matrix to linearize the dynamical system. Let the following be defined as functions: $f_1(p_s,p_i,z) = p_s$, $f_2(p_s,p_i,z) = p_i$, and $f_3(p_s,p_i,z) =$. By setting $q_s = \nu_s(1-\sigma_s)$, $q_i = \nu_i(1-\sigma_i)$, and $Q = 1+h(q_s p_s + q_i p_i) + \tau z$, the Jacobian matrix J is denoted by the following matrix:

$$J = \begin{pmatrix} r\left(1-\frac{2p_s+p_i}{K}\right) - \beta p_i - \frac{q_s z(1+hq_i p_i+\tau z)}{Q^2} & -\frac{rp_s}{K} - \beta p_s + \frac{q_s q_i p_s h z}{Q^2} & -\frac{q_s p_s(1+hq_s p_s+hq_i p_i)}{Q^2} \\ \beta p_i + \frac{q_s q_i h p_i z}{Q^2} & \beta p_s - (\phi_i+\rho) - \frac{q_i z(1+hq_s p_s+\tau z)}{Q^2} & -\frac{q_i p_i(1+hq_s p_s+hq_i p_i)}{Q^2} \\ \frac{\zeta z q_s(1+\tau z)}{Q^2} & \frac{\zeta z q_i(1+\tau z)}{Q^2} & -\delta + \frac{\zeta(q_s p_s+q_i p_i)(1+hq_s p_s+hq_i p_i)}{Q^2} \end{pmatrix}. \tag{6}$$

The local stability analysis of all the equilibrium points listed above are carried out by substituting their values into the Jacobian matrix in order to obtain the eigenvalues of the matrix.

Theorem 4. The equilibrium point B_0 is unstable.

Proof. The Jacobian J evaluated at B_0 is a diagonal matrix with the eigenvalues of $\lambda_1 = r$, $\lambda_2 = -(\phi_i+\rho)$, and $\lambda_3 = -\delta$. Since $r > 0$, one eigenvalue is positive while two are negative. Hence, the equilibrium point B_0 is an unstable saddle point. This signifies that extinction is prevented by the prey growth. □

Theorem 5. B_1 is asymptotically stable if $R_0 < 1$ and $R_0^z < 1$.

Proof. The Jacobian matrix evaluated at B_1 is upper triangular matrix:

$$\begin{pmatrix} -r & -(r+\beta K) & -\frac{q_s K}{1+hq_s K} \\ 0 & \beta K-(\phi_i+\rho) & 0 \\ 0 & 0 & -\delta+\frac{\zeta q_s K}{1+hq_s K} \end{pmatrix}. \quad (7)$$

The eigenvalues of the disease-free equilibrium point B_1 are computed to be $\lambda_1 = -r$, $\lambda_2 = \beta K - (\phi_i + \rho)$, and $\lambda_3 = \frac{\zeta q_1 K}{1+hq_1 K} - \tau$. Since $\lambda_1 = -r$, B_1 will be asymptotically stable if the disease's basic reproduction number (R_0) in the absence of predators $R_0 = \frac{\beta K}{\phi_i+\rho} < 1$ and the predator's baseline reproductive invasion threshold when entering a healthy prey system at carrying capacity $R_0^z = \frac{\zeta q_s K}{\delta(1+hq_s K)} < 1$. □

Theorem 6. B_2 is asymptotically stable if $R_1^z < 1$.

Proof. The Jacobian matrix evaluated at B_2 is obtained as

$$\begin{pmatrix} -\frac{rp_s^-}{K} & -\left(\frac{r}{K}+\beta\right)p_s^- & -\frac{q_s p_s^-}{Q^-} \\ \beta p_i^- & 0 & -\frac{q_i p_i^-}{Q^-} \\ 0 & 0 & \left[-\delta+\frac{\zeta(q_s p_s^- + q_i p_i^-)}{Q^-}\right] \end{pmatrix}. \quad (8)$$

The first eigenvalue is obtained from the third row $\lambda_3 = -\delta + \frac{\zeta(q_s p_s^- + q_i p_i^-)}{1+h(q_s p_s^- + q_i p_i^-)}$. For system to be asymptotically stable if $\lambda_3 < 0$ that is, $R_1^z = \frac{\zeta(q_s p_s^- + q_i p_i^-)}{\delta\left[1+h(q_s p_s^- + q_i p_i^-)\right]} < 1$. The remaining two eigenvalues (λ_1, λ_2) are computed by taking the determinant of the remaining 2×2 submatrix: $\lambda^2 + \left(\frac{rp_s^-}{K}\right)\lambda + \left(\frac{r}{K}+\beta\right)\beta p_s^- p_i^- = 0$. By the Routh-Hurwitz criteria for a second-order polynomial, $a_1 = \frac{rp_s^-}{K} > 0$ and $a_2 = \left(\frac{r}{K}+\beta\right)\beta p_s^- p_i^- > 0$. Therefore, B_2 is asymptotically stable if $R_1^z < 1$. □

Theorem 7. B_3 is asymptotically stable if $R_0(B_3) < 1$, $\eta_1 > 0$ and $\eta_2 > 0$.

Proof. The Jacobian matrix evaluated at B_3 is

$$J(B_3) = \begin{pmatrix} \frac{q_s z^-}{Q^-} - \frac{rp_s^-}{K} - \frac{q_s z^-(1+\tau z^-)}{(Q^-)^2} & -\frac{rp_s^-}{K} - \beta p_s^- + \frac{hq_s q_i p_s^- z^-}{(Q^-)^2} & -\frac{q_s p_s^-(1+hq_s p_s^-)}{(Q^-)^2} \\ 0 & \beta p_s^- - (\phi_i+\rho) - \frac{q_i z^-}{Q^-} & 0 \\ \frac{\zeta q_s z^-(1+\tau z^-)}{(Q^-)^2} & \frac{\zeta q_i z^-(1+\tau z^-)}{(Q^-)^2} & -\frac{\delta\tau z^-}{Q^-} \end{pmatrix}. \quad (9)$$

The first eigenvalue is obtained from the second row as $\lambda_2 = \beta p_s^- - (\phi_i+\rho) - \frac{q_i z^-}{1+hq_s p_s^- + \tau z^-}$. The effective basic reproduction number (R_0) for the disease in the presence of the predator population: $R_0(B_3) = \frac{\beta p_s^-}{(\phi_i+\rho)+\frac{q_i z^-}{1+hq_s p_s^- + \tau z^-}} < 1$.

The remaining two eigenvalues (λ_1, λ_3) are obtained by taking the determinant of the remaining 2×2 matrix: $\lambda^2 + \eta_1\lambda + \eta_2 = 0$, where $\eta_1 = \frac{rp_s^-}{K} + \frac{\delta\tau z^-}{Q^-} - \frac{hq_s^2 p_s^- z^-}{(Q^-)^2}$ and $\eta_2 = \frac{\delta\tau q_s (z^-)^2(1+\tau z^-)}{(Q^-)^3} + \frac{\zeta q_s^2 p_s^- z^-(1+hq_s p_s^-)(1+\tau z^-)}{(Q^-)^4} - \frac{r\delta\tau z^-}{D^-}\left(1-\frac{2p_s^-}{K}\right)$. B_3 is locally asymptotically stable if $R_0(B_3) < 1$, $\eta_1 > 0$ and $\eta_2 > 0$. □

Theorem 8. B_4 is asymptotically stable if the characteristic polynomial of the Jacobian matrix evaluated at B_4 satisfies the Routh-Hurwitz criteria for a third-order polynomial.

Proof. The main diagonal entries will be simplified using the equilibrium identities of the system ($\dot{p}_s = 0, \dot{p}_i = 0, \dot{z} = 0$). $\dot{p}_s = 0 \Rightarrow r\left(1-\frac{p_s^- + p_i^-}{K}\right) - \beta p_i^- = \frac{q_s z^-}{Q^-}$, $\dot{p}_i = 0 \implies \beta p_s^- - (\phi_i+\rho) = \frac{q_i z^-}{Q^-}$ and $\dot{z} = 0 \implies \delta = \frac{\zeta(q_s p_s^- + q_i p_i^-)}{Q^-}$. Substituting these identities back into the general Jacobian matrix gives:

$$J(B_4) = \begin{pmatrix} J_{11} & J_{12} & J_{13} \\ J_{21} & J_{22} & J_{23} \\ J_{31} & J_{32} & J_{33} \end{pmatrix},$$

where

$J_{11} = -\frac{rp_s^-}{K} + \frac{hq_s z^-(q_s p_s^- - q_i p_i^-)}{Q^{-2}}$,
$J_{12} = -\frac{rp_s^-}{K} - \beta p_s^- + \frac{hq_s q_i p_s^- z^-}{(Q^-)^2}$,
$J_{13} = -\frac{q_s p_s^-(1+hq_s p_s^- + hq_i p_i^-)}{Q^{-2}}$,
$J_{21} = \beta p_i^- + \frac{hq_s q_i p_i^- z^-}{Q^{-2}}$,
$J_{22} = \frac{hq_i z^-(q_i p_i^- - q_s p_s^-)}{Q^{-2}}$,
$J_{23} = -\frac{q_i p_i^-(1+hq_s p_s^- + hq_i p_i^-)}{Q^{-2}}$,
$J_{31} = \frac{\zeta q_s z^-(1+\tau z^-)}{Q^{-2}}$,
$J_{32} = \frac{\zeta q_i z^-(1+\tau z^-)}{Q^{-2}}$,

$J_{33} = -\frac{\delta\tau z^-}{Q^-}$.

The characteristic polynomial is $\lambda^3 + \eta_1\lambda^2 + \eta_2\lambda + \eta_3 = 0$ where $\eta_1 = -(J_{11} + J_{22} + J_{33}) = \frac{rp_s^-}{K} + -\frac{\delta\tau z^-}{Q^-}$, $\eta_2 = (J_{11}J_{22} - J_{12}J_{21}) + (J_{22}J_{33} - J_{23}J_{32}) + (J_{11}J_{33} - J_{13}J_{31})$, and $\eta_3 = -\det(J(B_4)) = -J_{11}(J_{22}J_{33} - J_{23}J_{32}) + J_{12}(J_{21}J_{33} - J_{23}J_{31}) - J_{13}(J_{21}J_{32} - J_{22}J_{31})$. If $\eta_1 > 0$, $\eta_3 > 0$ and $\eta_1\eta_2 - \eta_3 > 0$, B_4 is asymptotically stable. □

3.4.2 Global Stability Analysis of the Positive Equilibrium Point

Theorem 9. The coexistence equilibrium point $B_4 = (p_s^-, p_i^-, y)$ is globally asymptotically stable.

Proof. Consider the Lyapunov function $L(p_s, p_i, z)$ defined by

$$\begin{aligned} L(p_s, p_i, z) = &\left(p_s - p_s^- - p_s^- \ln\frac{p_s}{p_s^-}\right) \\ &+ c_1\left(p_i - p_i^- - p_i^- \ln\frac{p_i}{p_i^-}\right) \\ &+ c_2\left(z - z^- - z^- \ln\frac{z}{z^-}\right), \end{aligned} \tag{10}$$

where c_1, c_2 are weighing functions, $L(B_4) =$ and $\forall p_s, p_i, z \in \mathbb{R}^3 - \{B_4\}, L(p_s, p_i, z) > 0$. The derivative of (10) with respect to t gives

$$\begin{aligned} \frac{dL}{dt} = &\left(1 - \frac{p_s^-}{p_s}\right)\frac{dp_s}{dt} + c_1\left(1 - \frac{p_i^-}{p_i}\right)\frac{dp_i}{dt} \\ &+ c_2\left(1 - \frac{z^-}{z}\right)\frac{dz}{dt}. \end{aligned} \tag{11}$$

Substituting the system equations and the equilibrium identities into equation (11), we transform the matching terms into localized algebraic differences:

$$\begin{aligned} \frac{dL}{dt} = &-\frac{r}{K}(p_s - p_s^-)^2 - \frac{r}{K}(p_s - p_s^-)(p_i - p_i^-) \\ &- \beta(p_s - p_s^-)(p_i - p_i^-) \\ &- \nu_s(1-\sigma_s)\left(1 - \frac{p_s^-}{p_s}\right)\left(\frac{p_s z}{Q} - \frac{p_s^- z^-}{Q^-}\right) \\ &+ c_1\Bigg[\beta(p_s - p_s^-)(p_i - p_i^-) \\ &- \nu_i(1-\sigma_i)\left(1 - \frac{p_i^-}{p_i}\right)\left(\frac{p_i z}{Q} - \frac{p_i^- z^-}{Q^-}\right)\Bigg] \\ &+ c_2\zeta\left(1 - \frac{z^-}{z}\right)\Bigg[\frac{z\nu_s(1-\sigma_s)p_s}{Q} \\ &+ \frac{z\nu_i(1-\sigma_i)p_i}{Q} - \frac{z^-\nu_s(1-\sigma_s)p_s^-}{Q^-} \\ &- \frac{z^-\nu_i(1-\sigma_i)p_i^-}{Q^-}\Bigg] \end{aligned} \tag{12}$$

Setting $c_1 = 1$ and $c_2 = \frac{1}{\zeta}$ and simplifying gives coexistence equilibrium point gives

$$\begin{aligned} \frac{dL}{dt} = &-\frac{r}{K}(p_s - p_s^-)^2 - (\phi_i + \rho)(p_i - p_i^-)^2 \\ &- \delta(z - z^-)^2 \le 0. \end{aligned}$$

By applying LaSalle's Invariance Principle, every bounded trajectory starting in the positive octant $\mathbb{R}^3_+$ asymptotically approaches the equilibrium point B_4 as $t \to \infty$. Consequently, the interior coexistence equilibrium state B_4 is globally asymptotically stable. □

3.5 Transcritical Bifurcation

The transcritical bifurcation of the system (1) will be studied in this section. To study the transcritical bifurcation, we will make use of the Sotomayor's Theorem for transcritical bifurcation [32].

Theorem 10. Dynamical system (1) experiences transcritical bifurcation about B_1 where β is the parameter and the threshold value is $\beta_t^{[B_1]} = \frac{\phi_i + \rho}{K}$.

Proof. From Theorem 5, $\lambda_2 = \beta K - (\phi_i + \rho) \Rightarrow \beta_t^{[B_1]} = \frac{\phi_i + \rho}{K}$. The right and left eigenvectors are computed as $j = \begin{bmatrix} -\frac{r + \beta_c K}{r} & 1 & 0 \end{bmatrix}^T$ and $k = \begin{bmatrix} 0 & 1 & 0 \end{bmatrix}^T$ respectively. Let $G(p_s, p_i, z; \beta) = [g_1, g_2, g_3]^T$, the transcritical bifurcation's three conditions are evaluated as follows:

$$\begin{aligned} C_1 &= k^T G_\beta\left(B_1, \beta_t^{[B_1]}\right) \\ &= \begin{pmatrix} 0 & 1 & 0 \end{pmatrix}\begin{pmatrix} -p_s p_i \\ p_s p_i \\ 0 \end{pmatrix}_{(K,0,0)} \\ &= \begin{pmatrix} 0 & 1 & 0 \end{pmatrix}\begin{pmatrix} 0 \\ 0 \\ 0 \end{pmatrix} = 0. \end{aligned}$$

The bifurcation is not a saddle-node bifurcation since $C_1 = 0$. Next, we test for the second condition:

$$\begin{aligned} C_2 &= k^T[DG_\beta\left(B_1, \beta_t^{[B_1]}\right) j] \\ &= \begin{pmatrix} 0 & 1 & 0 \end{pmatrix}\begin{pmatrix} 0 & -K & 0 \\ 0 & K & 0 \\ 0 & 0 & 0 \end{pmatrix}\begin{pmatrix} -\frac{r + \beta_c K}{r} \\ 1 \\ 0 \end{pmatrix} \\ &= \begin{pmatrix} 0 & 1 & 0 \end{pmatrix}\begin{pmatrix} -K \\ K \\ 0 \end{pmatrix} = K. \end{aligned}$$

Since $K > 0$, $C_2 \neq 0$, hence the second condition

holds. Finally,

$$C_3 = k^T[D^2F_\beta\left(B_1;\beta_t^{[B_1]}\right)(j\cdot j)]$$
$$= \sum_{p,q=1}^{3}\frac{\partial^2 g_2}{\partial x_p\partial x_q}j_pj_q = \frac{\partial^2 g_2}{\partial p_s\partial p_i}j_1j_2$$
$$= -\frac{2\beta_t^{[B_1]}\left(r+\beta_t^{[B_1]}K\right)}{r}.$$

Since $\beta_t^{[B_1]}, r, K > 0$, $C_3 \neq 0$, hence the third condition holds. Since all three conditions of the Sotomayor's Theorem holds, the system exhibits transcritical bifurcation at B_1. □

Theorem 11. Dynamical system (1) experiences transcritical bifurcation about B_2 where δ is the parameter and the threshold value is $\delta_t = \frac{\zeta[\nu_s(1-\sigma_s)p_s^- + \nu_i(1-\sigma_i)p_i^-]}{1+h\left(\nu_s(1-\sigma_s)p_s^- + \nu_i(1-\sigma_i)p_i^-\right)}$.

Proof. From Theorem 6, $\lambda_3 = -\delta + \frac{\zeta[\nu_s(1-\sigma_s)p_s^- + \nu_i(1-\sigma_i)p_i^-]}{Q^-} \Rightarrow \delta_t = \frac{\zeta[\nu_s(1-\sigma_s)p_s^- + \nu_i(1-\sigma_i)p_i^-]}{1+h\left(\nu_s(1-\sigma_s)p_s^- + \nu_i(1-\sigma_i)p_i^-\right)}$. Using Jacobain matrix evaluated in B_2, the right eigenvector is computed as $j = [j_1 \quad j_2 \quad 10]^T$ where $j_1 = \frac{q_i}{\beta Q}$, $j_2 = -\frac{J_{11}j_1 + J_{13}}{J_{12}}$ while the left eigenvector $k = [0 \quad 0 \quad 1]^T$. Let $G(p_s, p_i, z; \beta) = [g_1, g_2, g_3]^T$, the transcritical bifurcation's three conditions are evaluated as follows:

$$C_1 = k^T G_\delta(B_2, \delta_t) = (0 \quad 0 \quad 1)\begin{pmatrix}0\\0\\0\end{pmatrix} = 0$$

The bifurcation is not a saddle-node bifurcation. Next, we test for the second condition:

$$C_2 = k^T[DG_\delta(B_2, \delta_t)\, j]$$
$$= (0 \quad 0 \quad 1)\begin{pmatrix}0 & 0 & 0\\0 & 0 & 0\\0 & 0 & -1\end{pmatrix}\begin{pmatrix}j_1\\j_2\\1\end{pmatrix}$$
$$= (0 \quad 0 \quad 1)\begin{pmatrix}0\\0\\-1\end{pmatrix} = -1.$$

Since $C_2 = -1 \neq 0$, the second condition holds. Finally,

$$C_3 = k^T[D^2F_\delta(B_2;\delta_t)(j\cdot j)] = \sum_{p,q=1}^{3}\frac{\partial^2 g_3}{\partial x_p\partial x_q}$$
$$= \frac{\partial^2 g_3}{\partial z^2} + 2\frac{\partial^2 g_3}{\partial p_s\partial z}j_1 + 2\frac{\partial^2 g_3}{\partial p_i\partial z}j_2$$
$$= \frac{2\zeta}{Q^2}(-\tau(q_sp_s^- + q_ip_i^-) + q_sj_1 + q_ij_2).$$

The third condition will be satisfied if $C_3 \neq 0$. Hence the Sotomayor's Theorem holds, the system exhibits transcritical bifurcation at B_2 □

Theorem 12. Dynamical system (1) experiences transcritical bifurcation about B_3 where β is the parameter and the threshold value is $\beta_t^{[B_2]} = \frac{1}{p_s^-}\left[\phi_i + \rho + \frac{\nu_i(1-\sigma_i)z^-}{1+h\nu_s(1-\sigma_s)p_s^- + \tau z^-}\right]$.

Proof. The proof is similar to Theorems 10 and 11 and it is omitted. □

4 Optimal Control Analysis

In this section, an optimal control analysis that stabilizes the dynamics of the eco-epidemiological population by reducing the infection rate and adjusting the interaction between prey and predators is described. The objective function $J(w_1, w_2, w_3)$ is formulated to minimize both the transmission costs and the lingering density of the infected population at the final time horizon T, thereby preventing an artificial end-of-horizon collapse of the control efforts. This objective function will be minimized to obtain the optimal policy for the controls $w = (w_1, w_2, w_3)$ over the time interval $[0, T]$, such that the state variables p_s, p_i, and z are solutions of (1) subject to the given initial conditions. Within this framework, treatment (w_1) and vaccination (w_2) play an important role in controlling the spread of disease by protecting individuals and lowering the overall rate of infection. Additionally, the controlw_3 denotes refuge enhancement measures such as expanding areas inaccessible to predators or providing alternative food sources [31], which reduce the encounter and interaction rates between prey and predators. All controls are assumed to be bounded within the closed interval $[0, 1]$. We introduce three time dependent variables $w_1(t)$, $w_2(t)$ and $w_3(t)$ to (1) as follows:

$$\begin{aligned}\dot{p_s} =& rp_s\left(1 - \frac{p_s + p_i}{K}\right) - (1-w_2)\beta p_sp_i \\ & - \frac{b_sp_sz}{Q},\\ \dot{p_i} =& (1-w_2)\beta p_sp_i - (\phi_i + \rho + w_1)p_i \\ & - \frac{b_ip_iz}{Q},\\ \dot{z} =& -\delta z + \frac{\zeta z[b_sp_s + b_ip_i]}{Q},\end{aligned} \tag{13}$$

where $b_s = \nu_s(1-\sigma_s-w_3)$ and $b_i = \nu_i(1-\sigma_i-w_3)$ and $Q = 1 + h(b_sp_s + b_ip_i) + \tau z$.

4.1 The Objective Functional in the Control Problem

Our purpose here is to identify the most effective set of controls $(w_1(t), w_2(t), w_3(t))$ that will reduce the cost of treatment and the number of infected prey $(p_i(t))$ as well as the rate of predation over a period of time interval $[0, T]$ to the barest minimum. In order to achieve this, we make use of the objective functional

$$J(w_1, w_2, w_3) = S_i p_i(T) + \int_0^T \left(a p_i(t) + \frac{1}{2} \sum_{j=1}^{3} c_j w_j^2 \right) dt,$$

subject to (13) where the term $S_i p_i(T)$ represents the terminal penalty (or scrap value) with a positive weight coefficient $S_i > 0$. This component explicitly penalizes the remaining density of the infected population at the final time T, ensuring that control interventions remain active and realistic up to the end of the time horizon. The parameter $a > 0$ is the weight constant, $c_j, j = 1, 2, 3$ are measures of the relative costs of the controls $w_j(t), j = 1, 2, 3$ and T is the terminal time. We will obtain the ideal control pair (w_1^*, w_2^*, w_3^*) such that for $(w_1, w_2, w_3) \in \Omega$

$$J(w_1^*, w_2^*, w_3^*) = \min J,$$

where Ω is the control set defined as

$$\Omega = \{(w_1, w_2, w_3) : 0 \leq w_j \leq 1, t \in [0, T], \; w_i \text{ is measurable}, j = 1, 2, 3\}.$$

4.2 Characterization of the Controls

Using the Pontryagin's minimum principle [33], we will obtain the optimal controls $w^* = (w_1^*, w_2^*, w_3^*)$ that gives the ideal minimal levels for the various cost functionals of (1).

Theorem 13. Let $U = (p_s, p_i, z)$ and $w = (w_1, w_2, w_3)$, suppose $(U^*(t), w^*(t))$ is an optimal control pair then there exists a nontrivial vector $m(t) = (m_1(t), m_2(t), m_3(t))$ that satisfies the following equations

$$\begin{aligned} m_1'(t) = &-m_1\left(r\left(1 - \frac{2p_s + p_i}{K}\right) - (1 - w_2)\beta p_i - \frac{b_s z(Q - h b_s p_s)}{Q^2}\right) \\ &- m_2\left((1 - w_2)\beta p_i + \frac{h b_s b_i p_i z}{Q^2}\right) \\ &- m_3\left(\frac{\zeta b_s z(1 + \tau z)}{Q^2}\right), \end{aligned} \tag{14}$$

$$\begin{aligned} m_2'(t) = a &+ m_1\left(\frac{r p_s}{K} + (1 - w_2)\beta p_s - \frac{h b_i b_s p_s z}{Q^2}\right) \\ &- m_2\Big((1 - w_2)\beta p_s - \phi_i - \rho - w_1 \\ &- \frac{b_i z(Q - h b_i p_i)}{Q^2}\Big) - m_3\left(\frac{\zeta b_i z(1 + \tau z)}{Q^2}\right), \end{aligned} \tag{15}$$

$$\begin{aligned} m_3'(t) = &\, m_3\delta + m_1\left(\frac{b_s p_s(Q - \tau z)}{Q^2}\right) \\ &+ m_2\left(\frac{b_i p_i(Q - \tau z)}{Q^2}\right) \\ &- m_3\left(\frac{\zeta(b_s p_s + b_i p_i)(1 + h(b_s p_s + b_i p_i))}{Q^2}\right). \end{aligned} \tag{16}$$

where $b_s = \nu_s(1 - \sigma_s - w_3)$, $b_i = \nu_i(1 - \sigma_i - w_3)$ and $Q = 1 + h(b_s p_s + b_i p_i) + \tau z$. The updated transversality conditions are given by:

$$m_1(T) = 0, \quad m_2(T) = S_i, \quad m_3(T) = 0, \tag{17}$$

and the optimal controls are characterized as:

$$\begin{aligned} w_1^* &= \min\left(1, \max\left(0, \frac{m_2 p_i}{c_1}\right)\right), \\ w_2^* &= \min\left(1, \max\left(0, \frac{\beta p_s p_i(m_2 - m_1)}{c_2}\right)\right), \\ w_3^* &= \min\Bigg(1, \max\Bigg(0, \frac{1}{c_3 Q^2}\Big[m_1 p_s z\big(\nu_s Q \\ &\quad - h b_s(\nu_s p_s + \nu_i p_i)\big) \\ &\quad + m_2 p_i z\big(\nu_i Q - h b_i(\nu_s p_s + \nu_i p_i)\big) \\ &\quad - m_3 \zeta z(\nu_s p_s + \nu_i p_i)(1 + \tau z)\Big]\Bigg)\Bigg). \end{aligned} \tag{18}$$

Proof. We will commence by writing out the Lagrangian and Hamiltonian. The Lagrangian is denoted as

$$\begin{aligned} &\mathcal{L}(p_s, p_i, z, w_1, w_2, w_3) \\ &\qquad = a p_i(t) + \frac{c_1 w_1^2 + c_2 w_2^2 + c_3 w_3^2}{2}, \end{aligned}$$

and the Hamiltonian is

$$\mathcal{H} = ap_i(t) + \frac{c_1w_1^2 + c_2w_2^2 + c_3w_3^2}{2} + m_1\left(rp_s\left(1 - \frac{p_s + p_i}{K}\right) - (1 - w_2)\beta p_s p_i - \frac{b_s p_s z}{Q}\right) + m_2\left((1 - w_2)\beta p_s p_i - (\phi_i + \rho + w_1)p_i - \frac{b_i p_i z}{Q}\right) + m_3\left(-\delta z + \frac{\zeta z[b_s p_s + b_i p_i]}{Q}\right).$$

By the Pontryagin's Maximum Principle, the adjoint variables satisfy the system of differential equations given by:

$$m_1'(t) = -\frac{\partial \mathcal{H}}{\partial p_s},\ m_2'(t) = -\frac{\partial \mathcal{H}}{\partial p_i},\ m_3'(t) = -\frac{\partial \mathcal{H}}{\partial z}. \tag{19}$$

Using (19), we obtain (14) − (16) with transversality conditions state in (17). Finally, we obtain the controls $(w_j^*, j = 1, 2, 3)$ that minimizes the Hamiltonian by setting the partial derivative of the Hamiltonian with respect to $w_j, j = 1, 2, 3$ in Ω equal to zero to obtain:

$$\frac{\partial \mathcal{H}}{\partial w_1} = c_1w_1 - m_2p_i = 0 \Rightarrow w_1 = \frac{m_2p_i}{c_1},$$

$$\frac{\partial \mathcal{H}}{\partial w_1} = c_2w_2 + \beta p_s p_i(m_1 - m_2) = 0 \Rightarrow w_2 = \frac{\beta p_s p_i(m_1 - m_2)}{c_2},$$

and

$$\frac{\partial \mathcal{H}}{\partial w_1} = c_3w_3 + m_1\left(\frac{Q\nu_s p_s z - b_s p_s z h[v_s p_s + v_i p_i]}{Q^2}\right) + m_2\left(\frac{Q\nu_i p_i z - b_i p_i z h[v_s p_s + v_i p_i]}{Q^2}\right) + m_3\left(\frac{\zeta z(\nu_s p_s + \nu_i p_i)(-Q + h[b_s p_s + b_i p_i]}{Q^2}\right) = 0.$$

By the operational bounds [0,1], (18) is obtained. □

5 Numerical Simulation

In this section, we will numerically validate the results that been obtained analytically. Our data selection is based on the ranges in [34]. The numerical integration of the eco-epidemiological system (1) and its corresponding optimal control formulation (13) is performed using the fourth-order Runge-Kutta scheme and the forward-backward sweep method. While our primary focus centers on exploring the properties of transcritical bifurcations and multi-strategy optimal controls, we commence this section with an evaluation of the system's structural stability.

5.1 Stability

To validate the convergence and stability of (1), we use the following parameter set ($r = 1.5$, $K = 10.0$, $\beta = 0.6$, $\phi_i = 0.4$, $\rho = 0.2$, $h = 0.1$, $\tau = 0.2$, $\zeta = 0.4$, $\nu_s = 0.5$, $\sigma_s = 0.2$, $\nu_i = 0.6$, $\sigma_i = 0.1$, $\delta = 0.3$. By this parameters, the equilibrium points B_0, B_1, B_2 and B_3 are all unstable while B_4 satisfies the Routh-Hurwitz criteria and is locally asymptotically stable. Figure 1 Appendix $A.1$ shows the path transitions from B_0, B_1, B_2, and B_3 to B_4, respectively. To confirm the global asymptotic stability proven via the Lyapunov direct method, Figure 2(a)-(c) Section $A.1$ displays the time-series convergence of susceptible prey, infected prey, and predators across multiple disparate initial states while Finally, Figure 2(d) Appendix $A.1$ maps these paths into a comprehensive three-dimensional phase portrait, visually anchoring the global basin of attraction surrounding B_4.

5.2 Bifurcations

Figure 3(a)-(b)Appendix $A.2$ shows the spread of a disease within a population as the β passes the threshold value $\beta_t^{[B_1]} = 0.003$, the susceptible prey population drops below carrying capacity as a lingering endemic state emerges, while the population of the infected prey increases. The stable equilibrium point B_1 becomes unstable and settles into a new equilibrium point. Figure 4 Appendix $A.2$ is a phase portrait showing change in its topological nature from stable sink to saddle point. When $\beta < \beta_t^{[B_1]}$, no matter the population of infected prey, the trajectories are forced back into B_1, but when $\beta > \beta_t^{[B_1]}$, the trajectory is pulled away toward endemicity even for tiny population of infected prey.

Figure 5 Appendix $A.2$ shows the bifurcation diagram for B_2 when $\delta < \delta_t \approx 1.66$, the predator invades successfully, while the predator dies off when $\delta > \delta_t \approx 1.66$. Introducing a predator causes the population of healthy prey (p_s) to increase as the predator acts as biological control agent by suppressing the infected prey (p_i) and keeping the disease transmission level low in the system. Figure 6(a) and (c) Appendix $A.2$ shows that the subcritical case in the (p_s, p_i) phase plane exhibits a bi-stability. B_2 remains stable, but it is surrounded by a region

bounded by an unstable coexistence saddle point (B_3). If initial conditions cross outside this boundary, the trajectories are drawn toward a larger, fully stable interior coexistence equilibrium (B_4). In the supercritical case, the equilibrium point B_2 is unstable. There is no bi-stability but the trajectories are drawn into the global basic of attraction of B_4.
Figure 7 Appendix $A.2$ is the bifurcation diagram for the equilibrium point B_3. It is observed that the system undergoes both transcritical and Hopf-bifurcations wtih threshold values $\beta_t^{[B_3]} = 0.08$ and $\beta_H^{[B_3]} = 0.65$ respectively. At very low transmission rate, (β), the infection is not able establish it self in the ecosystem, but as $\beta \geq \beta_t^{[B_3]} = 0.08$, the disease begins to take hold forcing the system to move from the stable B_3 to B_4 where the susceptible prey and the predators reduce while the infected prey increases. When $\beta \geq \beta_H^{[B_3]} = 0.65$, the system losses its stability and experiences massive oscillation causing the prey populations to drop to the level that the predators face the risk of extinction.
Figure 8(a) Appendix $A.2$ the transmission rate is low and the infection cannot establish itself so the system transitions from a limit cycle to a stable equilibrium point. In Figure 8(b) Appendix $A.2$ The transmission rate is between the ($\beta_t^{[B_3]} < \beta = 0.35 < \beta_H^{[B_3]}$) the populations initially fluctuate, because the disease spreads moderately, it acts as a natural brake. It thins the prey population just enough to prevent overwhelming predator, but not enough to cause host collapse. Figure 8(c) Appendix $A.2$ show the system behaviour when the transmission rate $\beta = 0.80$ is above the Hopf bifurcation threshold ($\beta_H = 0.65$), the system does not settle into a static equilibrium point. Instead, it displays periodic limit cycles where the three populations perpetually chase each other in staggered wave peaks.

5.3 Optimal Control

The numerical simulations of the eco-epidemiological model under the proposed optimal control strategies is presented in this section. To analyze the structural impact of the terminal penalty on the control dynamics, we used the following ecological and epidemiological parameters set ($r = 1.5$, $K = 40.0$, $\beta = 0.45$, $\phi_i = 0.1$, $\rho = 0.1$, $\delta = 0.2$, $\zeta = 0.3$, $h = 0.05$, $\tau = 0.02$, $\nu_s = 0.3$, $\sigma_s = 0.1$, $\nu_i = 0.2$, $\sigma_i = 0.05$). The initial conditions are initialized at $p_s(0) = 20.0$, $p_i(0) = 10.0$, and $z(0) = 5.0$. The weight coefficients within the objective functional are chosen as $a = 0.25$, $c_1 = 2.0$, $c_2 = 3.0$, and $c_3 = 4.0$. Figure 9(a) Appendix $A.3$ shows the dynamics of the system when there is no management control, as the infection spreads at a high rate, the density of the infected population rises sharply and crashes to zero as the population of the susceptible decreases this causes the predator density to steadily diminish. The varying amplitude graph oscillation are an indication that the population fluctuates continuously over time. Figure 9(b) Appendix $A.3$ shows the system when management control measures are applied. During the uncontrolled regime, the epidemic explodes, destabilizing the prey and driving the into a severely depleted, low-density state, the management control successfully flattens the infection curve and protects the system until it is stopped, then the system experiences a relapse of the infection. In Figure 9(c) Appendix $A.3$, as a result of the high penalty of $S_i = 1000$ set, the system has moved from a short-sighted budget saving operation to an aggressive eradication system. At the end of the control management phase the disease has been eradicated and system transitions into a stable disease-free, thriving predator-prey environment.
Figure 10 Appendix $A.3$ is a control profile of the system showing how the optimization algorithm balances the cost against ecological benefits. In 10(a) both w_1 and w_2 start high to mitigate the effect of the infection, while w_1 gradually slopes down w_2 stays consistently high to maintain a defensive barrier. w_3 fluctuates depending on the densities of the predator and healthy prey. All the three controls drop to zero simultaneously before $t = 20$ in order to save cost as there is no terminal penalty attached the result of this is a latent disease reservoir survive leading to a relapse of the infection after the control regime is over. When a high terminal economic penalty ($S_i = 1000$) is attached to the system, the optimizer ensures that the infection is eradicated before the end of the management window 10(b) Appendix $A.3$. Figure 11 Appendix $A.3$ on the other hand shows a comparative analysis of the disease control strategies individually and combined.

6 Conclusion

In this study, we formulated and analyzed an eco-epidemiological prey-predator model that accounts for resource competition, disease transmission among prey, a Beddington-DeAngelis functional response, and a constant prey refuge. The well-posedness of the model was established through proofs of existence, uniqueness, non-negativity, and uniform boundedness of the dynamical trajectories. The stability for five ecological equilibria was obtained, culminating in the proof of global asymptotic stability for the coexistence state via LaSalle's Invariance Principle. We also proved that changes in important parameters, such as the disease transmission rate and predator mortality rate, trigger transcritical bifurcations that dynamically alter the

system's topological landscape.
The implementation of optimal control theory yielded vital insights for conservation and habitat management. By treating vaccination, treatment, and refuge expansion as dynamic control variables, we characterized the optimal intervention policies via the Hamiltonian framework. Our numerical simulations showed a significant management trade-off. Budget-saving management strategies result in a latent disease reservoir that triggers a severe infection relapse once controls are lifted, while assigning a substantial terminal economic penalty shifts the optimizer toward aggressive eradication. This intervention successfully flattens the infection curve permanently, establishing a stable, disease-free, and balanced predator-prey ecosystem.

Acknowledgment:
The authors are grateful to the reviewers for their suggestions.

References:

[1] K. Q. Khalaf, A. A. Majeed, and R. K. Naji. "The local bifurcation and the hopf bifurcation for eco-epidemiological system with one infectious disease," Gen, vol. 31, no. 1, pp. 18-41, 2015.

[2] R. K. Naji and R. A. Hamodi, "The dynamics of an ecological model with infectious disease," Glob. j. eng. sci. res., vol. 3, no. 8, pp. 69–89, 2016.https://doi.org/10.5281/zenodo.61221

[3] S. Kumar and H. Kharbanda, "Stability analysis of prey- predator model with infection, migration and vaccination in prey," 2017, https://arxiv.org/abs/1709.10319

[4] S. P. Bera, A. Maiti, and G. P. Samanta, "A prey-predator model with infection in both prey and predator," Filomat, vol. 29, no. 8, pp. 1753–1767, 2015.https://doi.org/10.2298/FIL1508753B

[5] C. Ji, and D. Jiang, "Analysis of a predator-prey model with disease in the prey," Int. J. Biomath., vol. 6, iss. 3, 1350012, 2013. https://doi.org/10.1142/S1793524513500125

[6] S. Roy, S. Samanta, H. Nayak and P.K. Tiwari, "Deterministic vs. stochastic dynamics of a predator-prey system with disease in prey: Impact of fear and supplementary foods," Int. J. Biomath. 2450047 (2024). https://doi.org/10.1142/S1793524524500475

[7] D. Greenhalgh and M. Haque, "A predator-prey model with disease in the prey species only," Math. Methods Appl. Sci., 30(8) (2007), pp. 911–929. https://doi.org/10.1002/mma.815

[8] E. Venturino, "Epidemics in predator-prey models: disease in the predators," Math. Med. Biol., vol. 19, iss. 3, pp. 185–205, 2022. https://doi.org/10.1093/imammb/19.3.185.

[9] B.W. Kooi, G.A. van Voorn, and K.P. Das, "Stabilization and complex dynamics in a predatorprey model with predator suffering from an infectious disease," Ecol. Complex. vol. 8, iss. 1, 113122, 2011. https://doi.org/10.1016/j.ecocom.2010.11.002.

[10] J. P. Tripathi, S. Tyagi, and S. Abbas, "Global analysis of a delayed density dependent predator–prey model with Crowley–Martin functional response," Commun. Nonlinear Sci. Numer. Simul., vol. 30, iss.1-3, pp. 45-69, 2016. https://doi.org/10.1016/j.cnsns.2015.06.008

[11] L. N. Guin, P. J. Pal, J. Alzahrani, N. Ali, K. Sarkar, S. Djilali, A. Zeb, I. Khan, and S. M. Eldin, "Influence of Allee effect on the spatiotemporal behavior of a diffusive predator–prey model with Crowley–Martin type response function," Sci. Rep., vol. 13, iss. 1, 2023. https://doi.org/10.1038/s41598-023-28419-0

[12] B. Tiwari, and S. N. Raw, "Dynamics of Leslie–Gower model with double Allee effect on prey and mutual interference among predators," Nonlinear Dyn., vol. 103, iss. 1, pp. 1229-1257, 2021. https://doi.org/10.1007/s11071-020-06095-3

[13] J. P. Tripathi, S. S. Meghwani, M. Thakur, and S. Abbas, "A modified Leslie–Gower predator-prey interaction model and parameter identifiability," Commun. Nonlinear Sci. Numer. Simul., vol. 54, pp. 331-346, 2018. https://doi.org/10.1016/j.cnsns.2017.06.005

[14] A. P. Maiti, B. Dubey, and J. Tushar, "A delayed prey–predator model with Crowley–Martin-type functional response including prey refuge," Math. Method. Appl. Sci., vol. 40, iss. 16, pp. 5792-5809, 2027. https://doi.org/10.1002/mma.4429

[15] M.A. Abbasi, R. Niaz, O. Albalawi, H. Alhazmi, H. A. E. Khalifa, "Dynamical analysis of an ecological model with prey refuge and Beddington–DeAngelis functional response," Stoch. Environ. Res. Risk Assess., vol 39, pp. 3827–3852, 2025. https://doi.org/10.1007/s00477-025-03039-4

[16] S. Samanta, R. Dhar, I. M. Elmojtaba, and J. Chattopadhyay, ”The role of additional food in a predator-prey model with a prey refuge,” J. Biol. Syst., vol. 24, iss. 02n03, pp. 345-365, 2016. https://doi.org/10.1142/s0218339016500182

[17] A. George Maria Selvam Selvam, R. Janagaraj, S. Britto Jacob, and D. Vignesh, ”Stability and bifurcations of a discrete-time prey-predator system with constant prey refuge,” J. Phys. Conf. Ser., vol. 2070, iss. 1, 012068, 2021. https://doi.org/10.1088/1742-6596/2070/1/012068

[18] Z. Liang, and X. Meng, ”Stability and Hopf bifurcation of a multiple delayed predator–prey system with fear effect, prey refuge and Crowley–Martin function,” Chaos, Solitons & Fractals, vol. 175, 113955, 2023. https://doi.org/10.1016/j.chaos.2023.113955

[19] W. Chen, H. Yu, C. Dai, Q. Guo, H. Liu, and M. Zhao, ”Stability and Bifurcation in a predator-prey model with prey refuge,” J. Biol. Syst., vol. 31, iss. 02, pp. 417-435, 2023. https://doi.org/10.1142/s0218339023500146

[20] Rajalakshmi Manoharan, Reenu Rani, Ali Moussaoui. Predator-prey dynamics with refuge, alternate food, and harvesting strategies in a patchy habitat[J]. Mathematical Biosciences and Engineering, 2025, 22(4): 810-845. doi: 10.3934/mbe.2025029

[21] M. S. Surendar, M. Sambath, K. Balachandran, and Y.-K. Ma, ”Qualitative analysis of a prey–predator model with prey refuge and intraspecific competition among predators,” Bound. Value Probl., vol. 2023, iss. 1, 2023. https://doi.org/10.1186/s13661-023-01771-w

[22] G. Tang, S. Tang, and R. A. Cheke, ”Global analysis of a Holling type II predator–prey model with a constant prey refuge,” Nonlinear Dyn., vol. 76, iss. 1, pp. 635-647, 2013. https://doi.org/10.1007/s11071-013-1157-4

[23] P. K. Santra, G. S. Mahapatra, and G. R. Phaijoo, . ”Bifurcation and Chaos of a Discrete Predator-Prey Model with Crowley–Martin Functional Response Incorporating Proportional Prey Refuge,” Math. Probl. Eng., vol. 2020, pp. 1-18, 2020. https://doi.org/10.1155/2020/5309814

[24] C. Cortés García, ”Bifurcations in a Leslie–Gower model with constant and proportional prey refuge at high and low density,” Nonlinear Anal. Real World Appl., vol. 72, 103861, 2023. https://doi.org/10.1016/j.nonrwa.2023.103861

[25] C. Mondal, D. Kesh, and D. Mukherjee, ”Bifurcation and global stability of a discrete prey-predator model with saturated prey refuge,” Math. Method Appl. Sci., vol. 46, iss. 17, pp. 18354-18374, 2023. https://doi.org/10.1002/mma.9562

[26] G. Hua, T. Yuan, S. Kaibiao, and S. Xinyu, ”Study on dynamic behavior of two fishery harvesting models: effects of variable prey refuge and imprecise biological parameters,” J. Appl. Math. Comput., vol. 69, iss. 6, pp. 4243-4268, 2023. https://doi.org/10.1007/s12190-023-01925-0

[27] H. Molla, S. Sarwardi, S. R. Smith, and M. Haque, Dynamics of adding variable prey refuge and an Allee effect to a predator–prey model. Alexandria Engineering Journal, 61(6), 4175–4188(2022). https://doi.org/10.1016/j.aej.2021.09.039

[28] J. Wang, X. Meng, L. Lv, J. Li, ”Stability and bifurcation analysis of a Beddington-DeAngelis prey-predator model with fear effect, prey refuge and harvesting,” Int. J. Bifurcation Chaos, vol. 33, pp. 2350013-221, 2023. https://doi.org/10.1142/S021812742350013X

[29] G. Koushik, and S. M. Partha, ”Bifurcation analysis of a prey–predator model with Beddington–DeAngelis type functional response and Allee effect in prey”, Int. J. Bifurcation Chaos, https://doi.org/10.1142/S0218127420502387

[30] S. Sudip, Y. K. Mahammad, and S. Prabir, ”Bifurcation analysis and optimal control in a predator-prey-infection model with additional food,” J. Innov. Appl. Math. Comput. Sci. vol 5, no. 2, pp. 219–252, 2025. doi:10.58205/jiamcs.v5i2.1956

[31] Derrick, W. R. and Grossman, S. I. . A first course in differential equations with applications. West Publishing Company.(1987). ISBN-10: 0314268952

[32] J. Sotomayor, Generic bifurcations of dynamical systems. In: Peixoto, M.M. (ed.) Dynamical Systems, pp 549–560. Academic Press, New York (1973). doi:10.1016/B978-0-12-550350-1.50047-3

[33] Lev Semenovisch Pontryagin, Mathematical Theory of Optimal Processes, Routledge, London, UK, 2018 https://doi.org/10.1186/s13661-023-01804-4

[34] S., Pareek, and R. Baghel, ”Nonlinear Dynamics of a Predator-Prey Model with Beddington-deAngelis Functional Response,” Int. J. Innov. Res. Anal., vol. 05, pp. 72–84, 2025. https://doi.org/10.62823/ijira/5.3(i).7790

Contribution of Individual Authors to the Creation of a Scientific Article (Ghostwriting Policy)

The authors equally contributed in the present research, at all stages from the formulation of the problem to the final findings and solution.

Sources of Funding for Research Presented in a Scientific Article or Scientific Article Itself

No funding was received for conducting this study.

Conflicts of Interest

The authors have no conflicts of interest to declare that are relevant to the content of this article.

Creative Commons Attribution License 4.0 (Attribution 4.0 International , CC BY 4.0)

This article is published under the terms of the Creative Commons Attribution License 4.0
https://creativecommons.org/licenses/by/4.0/deed.en_US

A Appendix: Figures

A.1 Stability

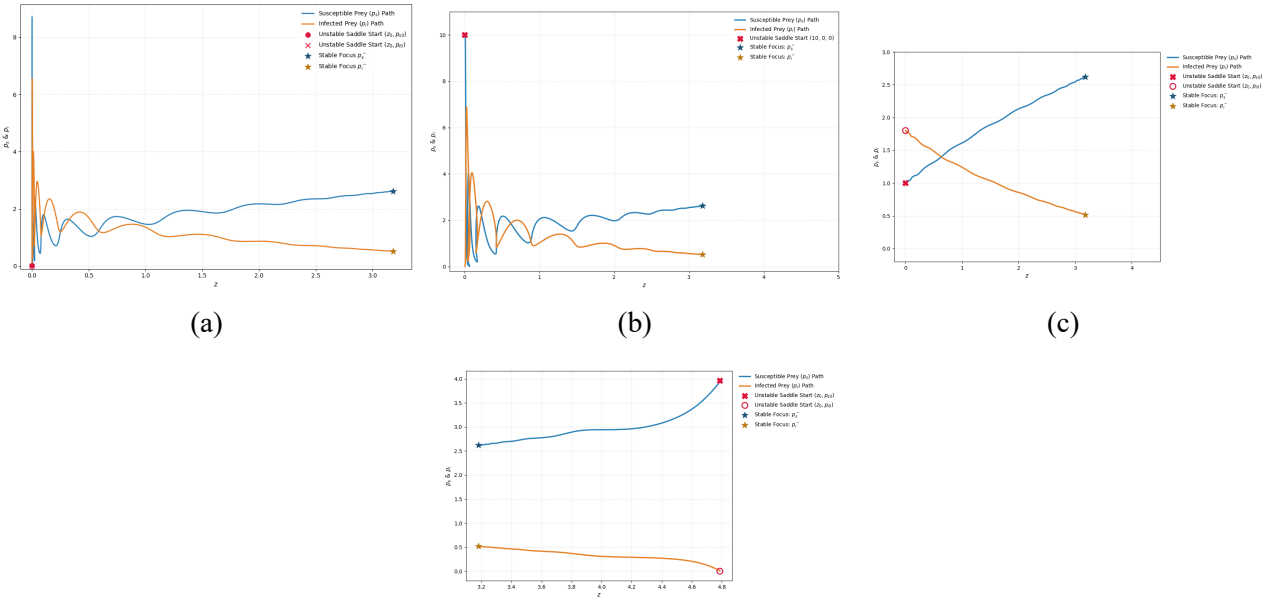

(a) (b) (c)

(d)

Figure 1: Transition form unstable equilibrium points to asymptotically stable coexistence equilibrium point. (a) System path from B_0 to B_4 (b) System path from B_1 to B_4 (c) System path from B_2 to B_4 (d) System path from B_3 to B_4.
Source: Created by the authors.

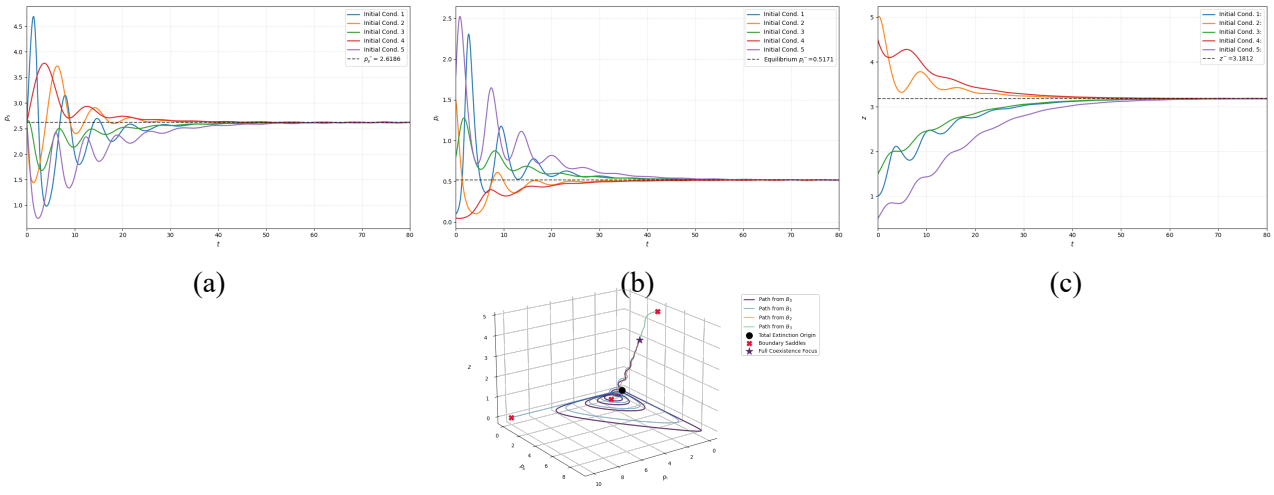

(a) (b) (c)

(d)

Figure 2: Convergence to the asymptotically stable coexistence equilibrium point using different initial conditions. (a) Susceptible prey convergence (b) Infected prey Convergence (c) Predator Convergence (d) Phase portrait of convergence from different paths.
Source: Created by the authors.

A.2 Bifurcations

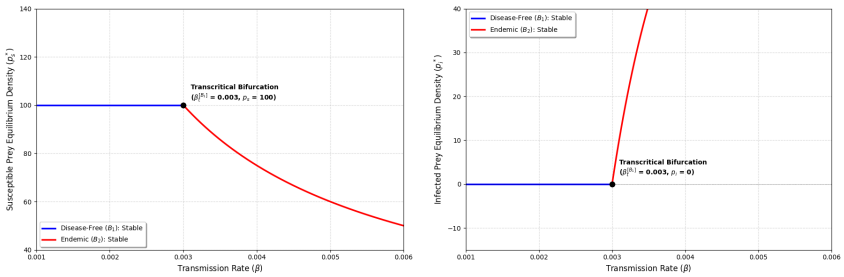

(a) (b)

Figure 3: Transcritical bifurcation sweep diagrams of system (1) at B_1 with parameter values $r = 1.00$, $K = 100.00$, $\phi_i = 0.2$, $\rho = 0.1$. (a) β against Susceptible prey (b) β against Infected prey.
Source: Created by the authors.

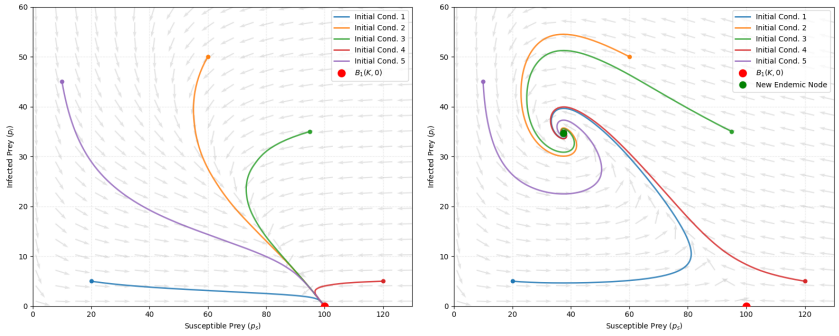

(a) (b)

Figure 4: Transcritical bifurcations phase portrait of system (1) at B_1 with parameter values $r = 1.00$, $K = 100.00$, $\phi_i = 0.2$, $\rho = 0.1$. (a) Subcritical case $\beta = 0.0015 < \beta_t^{[B_1]}$ (b) Supercritical case $\beta = 0.0080 > \beta_t^{[B_1]}$.
Source: Created by the authors.

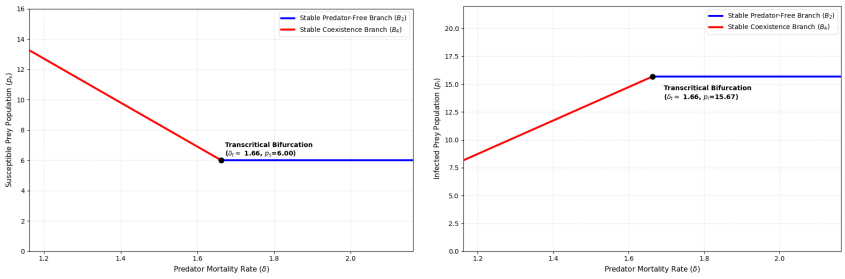

(a) (b)

Figure 5: Transcritical bifurcation sweep diagrams of system (1) at B_2 with parameter values $r = 1.00$, $K = 100.00$, $\phi_i = 0.1$, $\rho = 0.2$, $\beta = 0.05$, $\nu_s = 0.4$, $\nu_i = 0.2$, $\sigma_s = 0.1$, $\sigma_i = 0.1$, $h = 0.1$, $\tau = 0.1$, $\zeta = 0.5$ (a) δ against Susceptible prey (b) δ against Infected prey.
Source: Created by the authors.

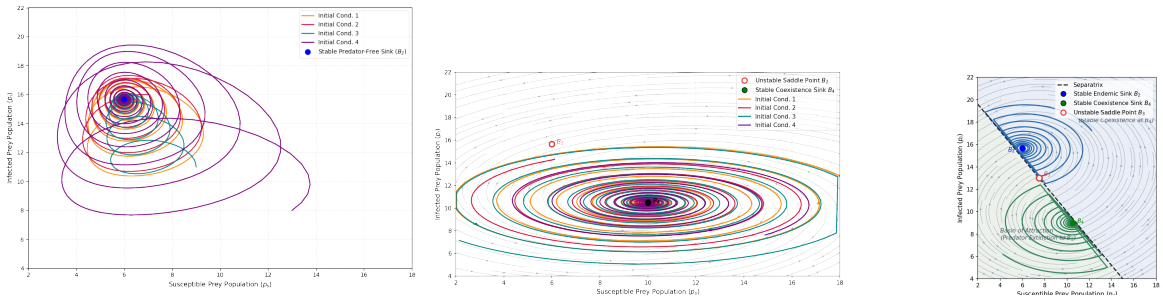

(a) (b) (c)

Figure 6: phase portrait of system (1) at B_2 with parameter values $r = 1.00$, $K = 100.00$, $\phi_i = 0.1$, $\rho = 0.2$, $\beta = 0.05$, $\nu_s = 0.4$, $\nu_i = 0.2$, $\sigma_s = 0.1$, $\sigma_i = 0.1$, $h = 0.1$, $\tau = 0.1$, $\zeta = 0.5$. (a) Subcritical case $\delta = 1.85 > \delta_t$ (b) Supercritical case $\delta = 0.080 < \delta_t$.
Source: Created by the authors.

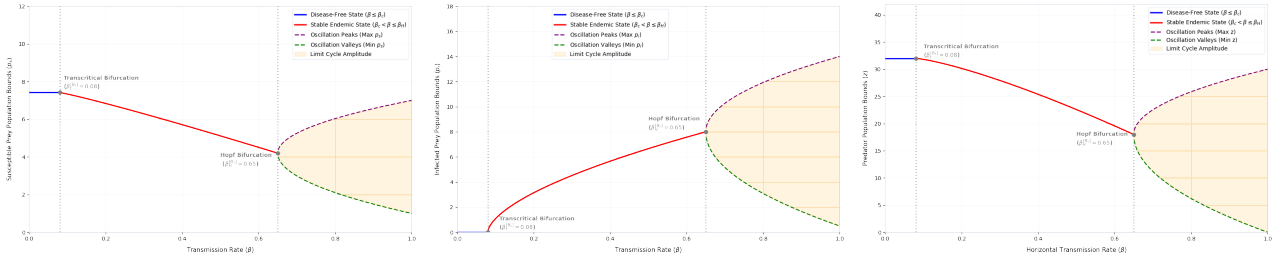

(a) (b) (c)

Figure 7: Full bifurcation diagram of system (1) at B_3 with parameter values $r = 2.00$, $K = 50.00$, $\phi_i = 0.25$, $\rho = 0.2$, $\nu_s = 0.3125$, $\nu_i = 0.2222$, $\sigma_s = 0.20$, $\sigma_i = 0.10$, $h = 0.05$, $\tau = 0.12$, $\zeta = 0.40$, $\delta = 1.15$. (a) Susceptible prey vs transmission rate (b) infected prey vs transmission rate (c) predators vs transmission rate.
Source: Created by the authors.

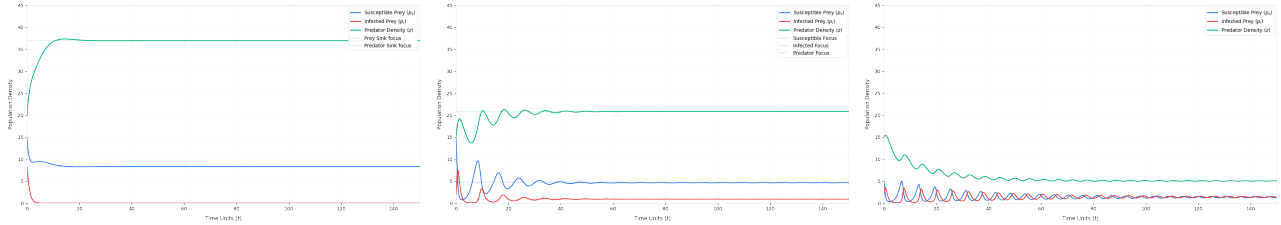

(a) (b) (c)

Figure 8: Time series analysis of system (1) at various value of β with parameter values $r = 2.00$, $K = 50.00$, $\phi_i = 0.25$, $\rho = 0.2$, $\nu_s = 0.3125$, $\nu_i = 0.2222$, $\sigma_s = 0.20$, $\sigma_i = 0.10$, $h = 0.05$, $\tau = 0.12$, $\zeta = 0.40$, $\delta = 1.15$. (a) $\beta = 0.05 < \beta_t^{[B_3]}$ (b) $\beta_t^{[B_3]} < \beta = 0.35 < \beta_H^{[B_3]}$ (c) $\beta = 0.80 > \beta_H^{[B_3]}$.
Source: Created by the authors.

A.3 Optimal Control

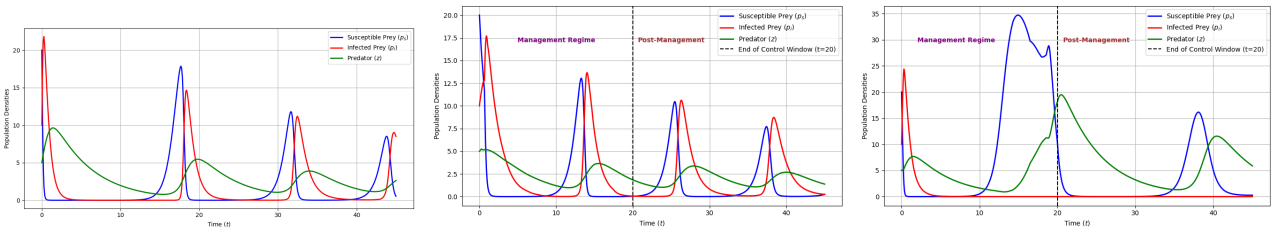

(a) (b) (c)

Figure 9: Time series analysis of system (1) without management controls ($c_1 = c_2 = c_3 = 0$) and with management controls ($c_1 = c_2 = 1.0, c_3 = 1.5$) and different penalties S_i (a) System without management controls (b) system with management control and without penalty ($S_i = 0$) (c) system with management control and without penalty ($S_i = 1000$).
Source: Created by the authors.

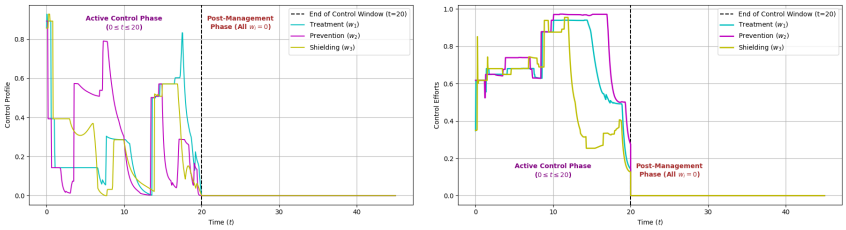

(a) (b)

Figure 10: Control profiles of the system (a) Control profile when there is no penalty ($S_i = 0$) (b) Control profile when there is penalty ($S_i = 1000$).
Source: Created by the authors.

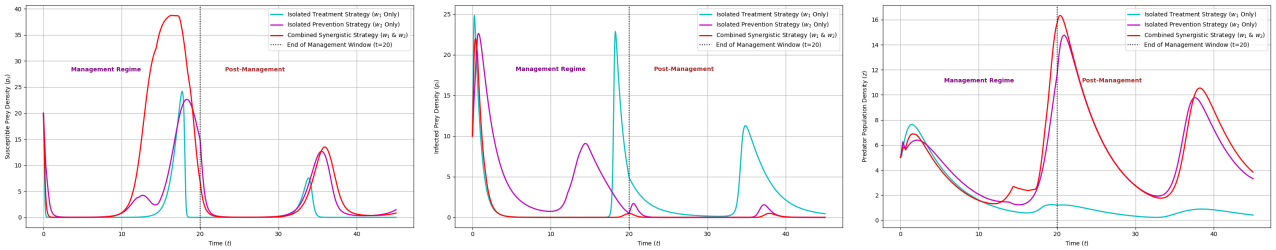

(a) (b) (c)

Figure 11: Comparative analysis of the disease control strategies on the populations when $S_i = 1000$ (a) susceptible preys (b) infected preys (c) predators.
Source: Created by the authors.